Pertanika J. Sci. & Technol. 25 (S): 189 - 196 (2017)

SCIENCE & TECHNOLOGY

Journal homepage: http://www.pertanika.upm.edu.my/

EFVD along Porcelain Insulator using the FEM

Kian Tsong Ho*, Mahdi Izadi and Mohd Zainal Abidin Ab Kadir

Centre for Electromagnetic and Lightning Protection Research (CELP), Faculty of Engineering, Universiti Putra Malaysia, Serdang, Malaysia

ABSTRACT

In this paper, cap and pin porcelain insulator was studied under an environment with different levels of humidity. The electric field strength and voltage distribution profile along the insulator string was simulated using a computational software package. In this study, ANSYS Maxwell based on the Finite Element Method (FEM) was used to simulate the short standard insulator string. The short standard insulator string was modelled as a five-unit cap and pin porcelain insulator that was stacked according to the IEC 60383 standard. Different humidity levels measured using relative humidity is applied to the insulator. From this simulation, the locations within the insulator under high electric field stress are identified when different humidity is applied.

Keywords: Porcelain Insulator, electric field strength distribution, humidity

INTRODUCTION

High quality outdoor insulators are needed to ensure the quality of the power transmitted over a transmission line, so research to improve the insulator is important. All insulators have to perform a dual task which is to mechanically hold up the transmission line and to electrically isolate the transmission line from the metal transmission tower. The history of insulators can be traced back to 1835, the first insulator was of a ceramic type. Since then, the ceramic type design has changed over the years with the increase in transmission system voltage. In 1960, a new type of insulator made of a polymer became available and this has since become popular (Looms, 1998). A polymer insulator is lighter and has better performance under conditions of pollution compared with the conventional ceramic insulator (Izadi, Rahman, Kadir, 2014). However, the ceramic insulator is still widely used due to its well-known field performance while the polymer insulator suffers from a lot uncertainty (Costea &

ARTICLE INFO

Article history:
Received: 24 August 2016
Accepted: 03 Jun 2017

E-mail addresses:
kiantsong@hotmail.com (Kian Tsong Ho),
aryphase@yahoo.com; mzk@upm.edu.my (Mahdi Izadi),
(Mohd Zainal Abidin Ab Kadir)
*Corresponding Author

ISSN: 0128-7680

Baran, 2012). In that case, a study of the porcelain insulator is important as there are many existing porcelain insulators still in service.

Previous research into the calculation of the electric field and potential distribution along a porcelain insulator includes the work of Reddy (Reddy et al., 2012) who applied the surface charge simulation method to study the surface field and potential distribution of normal and faulty insulator strings. Taklaja simulated a porcelain insulator in a distribution grid using COMSOL Multiphysics (Taklaja et al., 2015). Fouladi calculated the AC and transient potential distribution along a porcelain insulator under polluted conditions (Fouladi et al., 2014). Meanwhile, Gouda performed a laboratory test on a polluted overhead transmission line insulator under desert conditions (Gouda & Dein, 2013) while Kontargyri studied the electric field and voltage distribution along a porcelain insulator string by experimental work and simulation through the OPERA software (Kontargyri, Gonos & Stathopulos, 2009). Thus, it can be observed that many studies have investigated the effects of pollution on the electric field strength and voltage distribution, but not many on the effect of humidity alone on the electric field strength and voltage distribution around the insulator.

In this paper, the electric field distribution along a cap and pin porcelain insulator unit is simulated in an environment with different levels of humidity. Humidity is one of the factors that affect the flashover voltage of an insulator. However, the relation between different levels of humidity with the electric field and voltage distribution around the insulator remains unclear . Hence, this study was carried out by modelling the insulator string using ANSYS Maxwell. In the simulation, the insulator model is excited by AC power frequency of 50Hz under 27 %, 70 % and 90 % relative humidity; later, the electric field and the voltage distribution at different sections of the insulator are considered.

THE MODELLING AND SIMULATION METHOD

In this work, the insulator is simulated by ANSYS Maxwell software, the 2D model of the insulator is as shown in Figure 1.

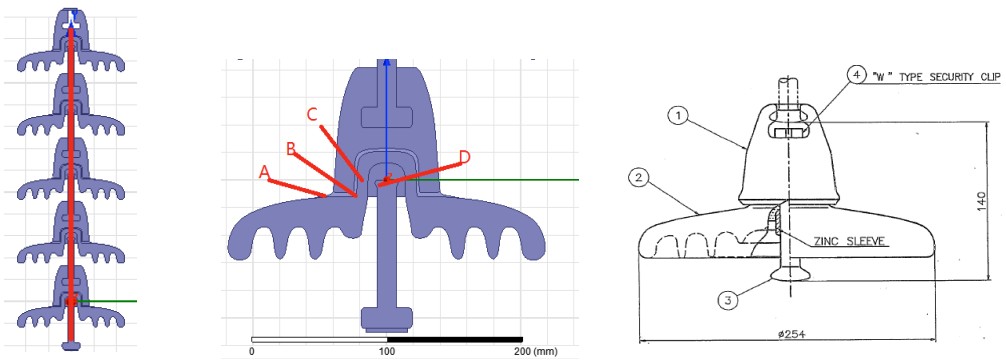

(a) (b) (c)

Figure 1. a) Cap and pin porcelain insulator unit; b) Point of interest in porcelain insulator model near energised end; c) Dimension of insulator model

Figure 1 shows one unit of a cap and pin porcelain insulator. The insulator string is stacked according to the line voltage. Hence, the higher the line voltage, the more insulator units are needed to be stacked up to withstand the applied voltage. In this study, the main focus is to investigate the effect of humidity on the electric field and voltage distribution on the cap and pin insulator. One cap and pin porcelain insulator is simulated to understand the relationship between humidity and electric field strength. However, it is advisable to test the high voltage insulator with a short standard string instead of a single unit insulator according to MS IEC 60383; thus, the insulator string to be modelled is a five- unit cap and pin porcelain insulator as shown in Figure 1(a) (MS IEC, 2013).

The computer used in this simulation is equipped with 16 GB ram and 2 processor core. The materials of the different parts of the insulator are defined first before the simulation begins. The relative permittivity of the cement and porcelain is 14 and 6 respectively (Asadpoor & Mirzaie, 2012). Before the simulation is started in the FEM modelling, the model undergoes a process known as meshing which discretises the insulator into small building blocks known as finite elements in a mesh which consists of triangles in 2D and tetrahedral in 3D. In this simulation, two thin electrodes are added to the top and bottom of the model to simulate the energised electrode and the ground electrode. In the energised electrode, the excitation voltage is applied according to the short standard string withstand voltage from data sheet of the porcelain insulator, so the AC power frequency voltage is set to 170 kV while the other electrode that simulates the ground is set to 0 V.

The points of interest to investigate the electric field on the porcelain insulator are shown in Figure 1(b) as A, B, C and D. These few points are chosen for investigation because on a sharp edge, the electric field strength will be intensified with a higher electric field strength compared with a flat surface. Thus, by observing these few points, the effect of humidity on the electric field distribution is more easily clarified. In order to investigate the effect of humidity on the electric field strength around the porcelain insulator, the simulation of the insulator model under different levels of humidity is undertaken using 27% RH, 70% RH and 90% RH. The first step is to determine the indoor environment humidity which acts as a reference. The average outdoor humidity on normal day in Malaysia is 70% RH, 90% RH representing a fog or dew day (Bowler & Abram, 2006; Rahman, Izadi & Kadir, 2014). As the relative humidity of air change, the permittivity of the air also changes. Thus, the relative humidity of the air can be simulated by assigning different relative permittivity to the air in the simulation. *In this work, the relative permittivity is obtained based on the following approach (Zarnik & Belavi, 2012):

$$\text{Relative permittivity} = \left[1 + \frac{211}{T}.\left(P + \frac{48.P_S}{T}\ .\ \text{RH}\right).\ 10^{-6}\right] \quad (1)$$

Where T is absolute temperature (k), p is (mm Hg) pressure of air, p_s (mm Hg) is pressure of saturated water vapour and RH is relative humidity (%)

RESULTS AND DISCUSSION

Electric field strength distribution around insulator model

Based on the simulation model shown in Figure 1, the 2D electric field strength contour plot around the porcelain insulator model near the energised end is shown in Figure 2.

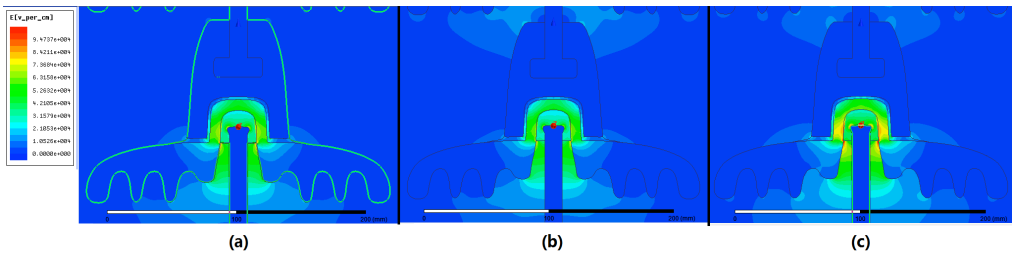

Figure 2. Electric field around the porcelain insulator model for a) 27% RH. b) 70% RH c) 90% RH

Figure 2 shows the electric field plot around the porcelain insulator for 27 % RH, 70 % RH and 90 % RH that is nearest to the energised electrode. It can be seen that the electric field strength is highest in the porcelain head portion cover inside the cap and is similar for three different humidity levels. This region suffers from high electric field strength and is at risk of corona discharge. Such discharge occurs in a location where the electric field strength exceeds the corona inception voltage of air which is roughly 30 $kVcm^{-1}$. From Figure 2, it can be observed that the area of blue is the region with a low electric field while the area in yellow green is the region with a high electric field. The points A and B are on the curve surface which is within the lower electric field (3 $kVcm^{-1}$ to 30 $kVcm^{-1}$) region compared with other parts of the insulator with an edge surface. Another part of the insulator that is of interest is the porcelain insulator head portion inside the cap which is point C in Figure 1(b). Based on Figure 2, point C has a high electric field of up to 80 $kVcm^{-1}$ when the applied relative humidity is 90 % RH. However, no obvious sharp edges are observed at that point in the model. The possible reason for the high electric field in this region is because of electric field intensification due to the sharp edge in the head of the pin or point D in Figure 1(b). The electric field strength of the various points in Figure 1(b) for different levels of relative humidity is tabulated in Table1.

Table 1
Electric field distribution at specific locations in the insulator near the energised end

Location	27 % RH ($kVcm^{-1}$)	70 % RH (kVcm-1)	90 % RH ($kVcm^{-1}$)
A	3	2	3
B	22	21	27
C	62	57	74
D	68	63	82

Based on Table 1, it is clear that the electric field strength decreases when the relative humidity increases from 27% to 70% RH. However, it increases when the relative humidity is further increased to 90% RH. Point A shows almost constant electric field strength for different relative humidity. Among the four points, point D shows the highest electric field strength which is at 68 $kVcm^{-1}$, 63 $kVcm^{-1}$ and 82 $kVcm^{-1}$ for relative humidity of 27%, 70% and 90% respectively. The possible reason for this is that point D is nearest to the energised end and has a pointy edge. Furthermore, in terms of relative humidity comparison, relative humidity of 90% shows the overall highest electric field strength. For instance, the electric field strength at point C with relative humidity of 90 % shows the highest value (74 $kVcm^{-1}$) followed by relative humidity of 70% (57 $kVcm^{-1}$) and relative humidity of 27% (62 $kVcm^{-1}$).

All locations show a big difference in electric field strength when simulated at the same relative humidity even though these locations are near to each other. For example, when the relative humidity is 90%, the electric field strength at point A is 3 $kVcm^{-1}$, and the electric field strength at point D is 82 $kVcm^{-1}$ at the same humidity level. This shows that the electric field strength around the porcelain insulator is highly uneven. Overall, there is no obvious trend for electric field when the relative humidity increases from 27% RH to 70% RH and 90% RH. However, when 90 % RH is applied, the electric field strength at all point inside the insulator head section is the highest for all four points A, B, C and D.

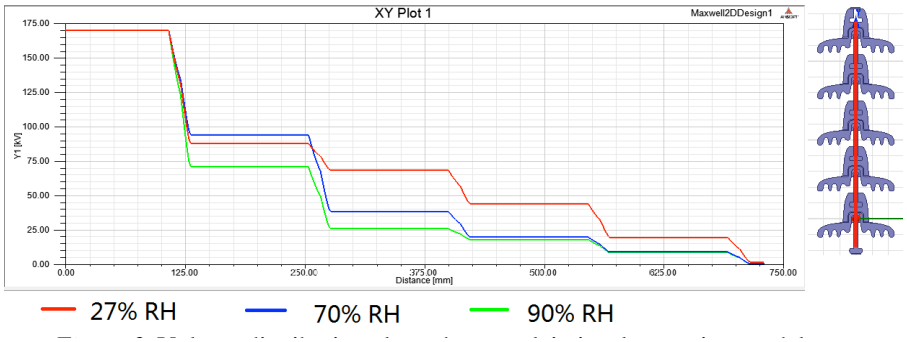

Figure 3. Voltage distribution along the porcelain insulator string model

Table 2
Voltage distribution along the porcelain insulator string

Relative Humidity (%RH)	0 mm (kV)	140 mm (kV)	280 mm (kV)	420 mm (kV)	600 mm (kV)
27	170	87	68	44	28
70	170	94	38	20	9
90	170	71	26	18	9

Voltage Distribution along the insulator string

Figure 3 provides a comparison of the voltage distribution along the cap and pin porcelain insulator string under different levels of humidity as shown by the mini model at the top right. The plot is drawn upwards, which means 0 mm is located at the bottom and 600 mm is located at the top. From Figure 3, it can be observed that in all relative humidity environments, the voltage along the insulator string shows the same shape which is a stair shape. Referring to Table 2 and taking the 27% RH plot as an example, the voltage at 0 mm shows 170 kV until it reaches the first cement and porcelain body part which is at the location of 125 mm. At that location, due to the resistance from the cement and porcelain part, the voltage drops from 170 kV to 87 kV, or a decrease of 48%. Point 140 mm is the cap of the first insulator near the energised end and the pin of the next insulator. The voltage in this region does not show an obvious change because the cap and pin of the porcelain insulator is made of stainless steel that has a low resistance so the voltage remains at 87 kV. At a point of 250 mm which is the cement and porcelain part of the second insulator from the energised end, the voltage drops from 87 kV to 68 kV, or a decrease of 21%. The voltage continues to drop at the 390 mm point from 68 kV to 44 kV, or a decrease of 35 %. At the point 690 mm, the cement and porcelain part of the last insulator causes the voltage distribution to drop from 12 kV to 0 kV. From the plot, it can be seen that in the cement and porcelain part of every insulator, the voltage distribution also drops, which can be observed at the points 130 mm, 260 mm, 390 mm and 550 mm and 690mm.

When the level of the relative humidity applied to the environment around insulator string is increased, the voltage distribution in the insulator string shows decreasing trend for all location except from point 125 mm to 250 mm when relative humidity (70%) is applied. At the 130 mm location, the 90% RH indicated the highest decrease from 170 kV to 71 kV or a 58% decrease. From the plot, it can be observed that the voltage distribution along the insulator is similar when the applied humidity is 27% RH and 70% RH from point 420 mm to 750 mm; the voltage distribution along the insulator has the same shape and almost similar value. The voltage distribution along the insulator string for 90% RH humidity is the lowest among the humidity applied along the whole insulator string; for example, at point 280mm, the voltage

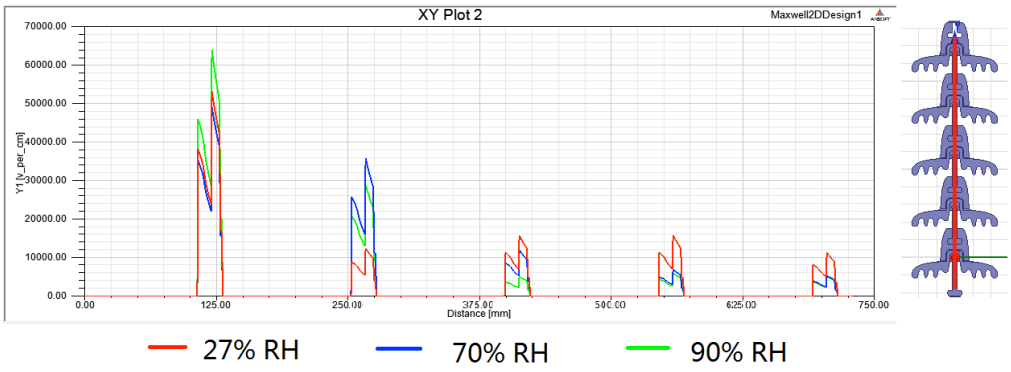

Figure 4. Electric field along the porcelain insulator model

Table 3
Electric field strength distribution along the insulator string

Relative humidity (%RH)	120 mm ($kVcm^{-1}$)	260 mm ($kVcm^{-1}$)	410 mm ($kVcm^{-1}$)	550 mm ($kVcm^{-1}$)	700 mm ($kVcm^{-1}$)
27	52	12	15	15	11
70	48	35	12	7	5
90	63	28	5	6	5

of the insulator for 27% is 68 kV, but the voltage distribution for the 90% RH environment is 26 kV only, which shows a decrease of 61% when humidity of environment changes from 27% RH to 90% RH. In the same location, the voltage distribution of 70% RH is 38 kV, which show a decrease of 31% when compared with 26 kV voltage distribution when the humidity applied is 90% RH.

Figure 4 shows the electric field distribution along the cap and pin porcelain insulator string under different levels of relative humidity. It can be observed that the electric field strength only exists at point where the cement and porcelain body part meet inside the cap of the insulator for each insulator in the insulator string. There are two peaks of electric field strength inside the cement and porcelain part of every insulator unit at the intersection between two different materials. The lower electric field peak is the intersection of stainless steel and cement while the higher electric field peak is due to the intersection of cement and porcelain. From the plot, it can be seen that the electric field strength distribution follows the same shape when the applied humidity differs. However, there is no obvious trend observed in the electric field strength when the humidity increases. Moreover, it can be seen from the plot that the electric field strength for all plots at every location is different although the same shape can be observed in every location. Referring to Table 2 it can be seen that the electric field strength is the highest at the 120 mm location when compared with the other locations of the insulator string. At a location of 120 mm, the electric field strength is 63 $kVcm^{-1}$ when the applied humidity is 90% RH, dropping to 48 $kVcm^{-1}$ when the applied humidity is 70% RH, but increased to 52 $kVcm^{-1}$ when the applied humidity is 27% RH. Along the insulator string, the electric field strength for 27% RH, 70% RH and 90% RH did not show any trend.

CONCLUSION

A systematic simulation work was conducted to study the electric field strength along the porcelain insulator using the finite element method. The developed model was used to predict the locations within the insulator under high stress due to the electric field. The locations surrounding the intersection and sharp edge points within the insulator were found to exhibit high electric field stress. In addition, the electric field strength near the sharp edge showed electric field strength intensification due to the effects of sharp edge. Hence, in order to reduce the electric field stress, the sharp edge should be replaced with a curved surface. This work shows the effect of relative humidity on the electric field and voltage distribution. even though the simulation only shows the very basic effect of different relative humidity level to electric field and voltage distribution around insulator. Future research can look at the effect

of relative humidity to porcelain insulator by investigating the effect of relative humidity to porcelain insulator in different perspective in order to have better understanding of the relative humidity effect.

REFERENCES

Asadpoor, M. B., & Mirzaie, M. (2012). Simulation and measurement of the voltage distribution on high voltage suspension Porcelain insulator string under pollution condition. *International Journal of Applied Sciences and Engineering Research, 1*(2), 165-175.

Bowler, N., & Abram, E. R. (2005). Monitoring the Effect of Relative Humidity During Curing on Dielectric Properties of Composites at Microwave Frequencies. In *AIP Conference Proceedings* (Vol. 820, No. A, p. 469). IOP Institute of Physics Publishing Ltd.

Costea, M., & Baran, I. (2012). a Comparative Analysis of Classical and Composite Insulators Behavior. *University" Politehnica" of Bucharest Scientific Bulletin, Series C: Electrical Engineering, 74*(1), 147-154.

Fouladi, R., Mirzaie, M., & Moradi, M. (2014). Calculation of AC and Transient Potential Distribution along HV Insulator String under Polluted Condition based on FEM. *International Journal of Engineering Innovation and Research, 3*(1), 74-78.

Gouda, O, E., & Dein, A. Z. E. (2013). Simulation of overhead transmission line insulators under desert environments. *IET Generation, Transmission & Distribution, 7*(1), 9-13.

Izadi, M., Rahman, M. A., & Ab Kadir, M. Z. A. (2014, March). On the voltage and electric field distribution along polymer insulator. In 2*014 IEEE 8th International Power Engineering and Optimization Conference (PEOCO2014)*.

Kontargyri, V. T., Gonos, I. F., & Stathopulos, I. A. (2009). Measurement and simulation of the electric field of high voltage suspension insulator. *European Transactions on Electrical Power, 19*(3), 509-517.

Looms, J. (1998). *Insulators for High Voltages*. London, United Kingdom: Peter Peregrinus Ltd.

MS IEC (2013). *Insulator for overhead lines with a nominal voltage above 1000 V*. MS IEC 60383.

R Rahman, M. A., Izadi, M., & Ab Kadir, M. Z. A. (2014, December). Influence of air humidity and contamination on electrical field of polymer insulator. In *IEEE International Conference on Power and Energy (PECon), 2014* (pp. 113-118). IEEE.

Reddy, B. S., Naik, B. S., Kumar, U., & Satish, L. (2012). Potential and electric field distribution in a ceramic disc insulator string with faulty insulators. *Properties and Applications of Dielectric Materials (ICPADM), 2012 IEEE 10th International Conference*. Bangalore.

Taklaja, P., Kiitam, I., Niitsoo, J., Kluss, J., & Hyvonen, P. (2015). Electric field distribution in glass and porcelain pin insulators. *Environment and Electrical Engineering (EEEIC), 2015 IEEE 15th International Conference*. IEEE.

Zarnik, M. S., & Belavi, D. (2012). An Experimental and Numerical Study of the Humidity Effect on the Stability of a Capacitive Ceramic Pressure Sensor. *Radioengineering, 21*, 201-206.